Neuron 50, 617–629, May 18, 2006 ©2006 Elsevier Inc. DOI 10.1016/j.neuron.2006.03.043

Visualizing the Cortical Representation of Whisker Touch: Voltage-Sensitive Dye Imaging in Freely Moving Mice

Isabelle Ferezou,[1] Sonia Bolea,[1] and Carl C.H. Petersen[1,*]
[1] Laboratory of Sensory Processing
Brain Mind Institute
SV-BMI-LSENS AAB 105
Station 15
Ecole Polytechnique Federale de Lausanne
CH-1015 Lausanne
Switzerland

Summary

Voltage-sensitive dye imaging resolves the spatiotemporal dynamics of supragranular subthreshold cortical activity with millisecond temporal resolution and subcolumnar spatial resolution. We used a flexible fiber optic image bundle to visualize voltage-sensitive dye dynamics in the barrel cortex of freely moving mice while simultaneously filming whisker-related behavior to generate two movies matched frame-by-frame with a temporal resolution of up to 2 ms. Sensory responses evoked by passive whisker stimulation lasted longer and spread further across the barrel cortex in awake mice compared to anesthetized mice. Passively evoked sensory responses were large during behaviorally quiet periods and small during active whisking. However, as an exploring mouse approached an object while whisking, large-amplitude, propagating cortical sensory activity was evoked by active whisker-touch. These experiments demonstrate that fiber optics can be used to image cortical sensory activity with high resolution in freely moving animals. The results demonstrate differential processing of sensory input depending upon behavior.

Introduction

Sensory information is processed in a highly distributed manner in the mammalian brain. Neocortical sensory processing can be imaged using voltage-sensitive dye (VSD), providing millisecond temporal resolution and subcolumnar spatial resolution (Grinvald et al., 1984; Orbach et al., 1985; Arieli et al., 1996; Kleinfeld and Delaney, 1996). Recent advances in imaging technology and new voltage-sensitive dyes (Shoham et al., 1999; Grinvald and Hildesheim, 2004) have allowed routine measurement of the spatiotemporal dynamics of sensory processing in head-fixed animals (Spors and Grinvald, 2002; Seidemann et al., 2002; Slovin et al., 2002; Petersen et al., 2003a, 2003b; Derdikman et al., 2003). Since the brain state and behavior likely affect sensory processing, it would clearly be important to be able to image cortical function in awake, freely moving animals, allowing a direct comparison of behavior, sensory input, and cortical activity. We therefore developed a technique for imaging cortical spatiotemporal dynamics in awake, freely moving mice using fiber optic image bundles. We focus on the processing of sensory input from the mystacial vibrissae which are represented in the primary somatosensory barrel cortex (Woolsey and Van der Loos, 1970). Using this technique, we analyzed differences in sensory responses between anesthetized and awake animals and during different behaviors in awake animals. We furthermore imaged the cortical representation of touch in real time as a mouse approached an object and made vibrissa contact.

*Correspondence: carl.petersen@epfl.ch

Results

Our goal was to develop a system for imaging both the whisker-related behavior and the spatiotemporal dynamics of barrel cortex in freely moving mice (Figure 1). Image transfer from the mouse to the epifluorescent imaging optics was achieved through the use of a fiber optic image bundle. The fiber was sufficiently light and flexible to allow the mice to move freely within a behavioral chamber. The flexibility of the fiber bundle derives from the assembly process, in which the fibers are only fused at the ends and left loose in the middle section. This allows the animal freedom to move and to turn around (see Movie S1 in the Supplemental Data).

Imaging Fluorescence with Fiber Optic Arrays

The fiber (Figures 2A–2C) was custom manufactured by Schott Fiber Optics based on their wound image bundle technology. The fibers were 50 cm long and had 8 μm cores with a numerical aperture of 0.6. The wound image bundle was prepared in a two-step process. Fibers were first assembled to form a multifiber array composed of 6 × 6 fibers (the multifibers can be seen in Figure 2A) and were then arranged into a 3 × 3 mm array containing 300 × 300 fibers (Figure 2B), forming a well-ordered array for coherent image transfer. The tip was enclosed in a nonmagnetic metal with a diameter of approximately 5 mm for mechanical stability (Figure 2C). This fiber tip was placed in direct contact with the cortical surface to achieve a high efficiency for emitting and collecting photons. The spatial resolution is limited by light scattering in the brain tissue.

Excitation light for fluorescence imaging can be brought to the cortical surface via the same fibers that detect the emission by using standard epifluorescence optics at the camera end of the fiber (Figure 1). To analyze how the excitation light penetrates into the cortex, we placed a single multifiber in direct contact with an in vitro brain slice of the mouse primary somatosensory cortex (Figure 2D). The end of the fiber nearer to the camera was illuminated with light of 630 nm. We imaged the brain slice using an Olympus 20× 0.95NA objective, mounted on a BX51WI microscope with a CoolSNAP HQ camera (Figure 2E). The penetration of the light into the brain slice was quantified from the photomicrograph by calculating contours of the normalized light intensity (Figure 2F). This excitation light penetrates the cortical layers 1, 2, and 3, with little reaching layer 4 or the infragranular layers. These measurements were made in

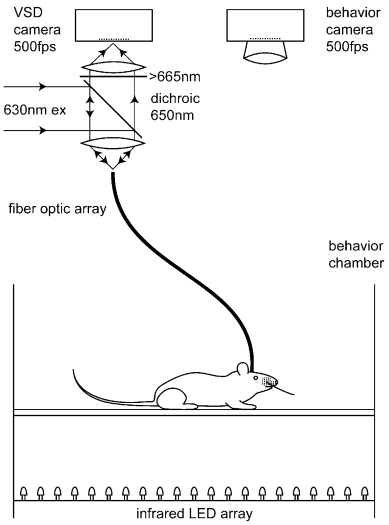

Figure 1. Voltage-Sensitive Dye Imaging and Filming of Behavior in Freely Moving Mice

The excitation light (630 nm) for fluorescence imaging was reflected using a dichroic mirror (650 nm) and focused onto the end of the fiber optic array with a 25 mm lens. The flexible fibers transferred the excitation light to the mouse cortex stained with voltage-sensitive dye RH1691. The emitted fluorescence was collected via the same optical pathway, long-pass filtered (>665 nm) and focused onto the high-speed camera sensor via a 135 mm lens. The fiber array was sufficiently light and flexible to allow the mouse to move freely within a behavior chamber. During the experiments, the chamber was illuminated from below by infrared LEDs. The silhouette of the mouse and its whiskers was filmed using another high-speed camera.

brain slices, which are largely exsanguinated. In vivo it is likely that the light penetration is further reduced through the light absorption of blood. The fiber imaging will therefore relate primarily to fluorescence in the supragranular layers. The light remained surprisingly confined laterally, suggesting that a reasonable horizontal spatial resolution might be achieved.

To analyze the lateral resolution of this fiber imaging technique, the tail vein was injected with ~100 μl of 1 mg/ml voltage-sensitive dye RH1691, and the fluorescence of the blood vessels was visualized via both standard optics (Figure 2H) and the fiber optic image bundle (Figure 2I). Both fluorescent images of the cortical surface blood vessels were very similar to the image of the blood vessels obtained with standard optics under green light illumination (Figure 2G). Even small surface vessels were clearly visible with the fiber fluorescence imaging. The horizontal spatial resolution of fluorescence deeper in the brain will, of course, be lower, but this is also true for conventional epifluorescence imaging. It is therefore important to know the depth of the fluorescence to be imaged.

The Voltage-Sensitive Dye RH1691 Preferentially Stains Layer 2/3

In this study we aimed to image the spatiotemporal dynamics of sensory processing using the voltage-sensitive dye RH1691. The dye can be topically applied to the craniotomy after removal of the dura. After staining for 1 hr, the cortical surface is extensively washed to remove unbound dye and then imaging can begin. In order to measure the penetration of RH1691 into the cortex, we fixed the brains of four mice with paraformaldehyde after imaging sessions and prepared 100 μm thick parasagittal slices (Figures 2J–2L). In four additional mice, we flash-froze the brain and prepared 20 μm thick cryosections to prevent any dye diffusion following the imaging experiment (Kleinfeld and Delaney, 1996). The dye penetration was not different when comparing the frozen cryosections and the paraformaldehyde-fixed slices (Figure 2L). Confocal imaging showed that RH1691 fluorescence was preferentially located in neocortical layer 2/3 (Figure 2J, individual experiment; Figure 2L, data from eight animals). The dye was excluded from intracellular compartments, leaving dark holes where neuronal cell bodies and large dendrites were located (Figure 2K). This is consistent with the dye staining and remaining on the outer plasma membrane of the cells in the brain tissue. Taken together with the data from Figures 2D–2I, it appeared likely that the fiber would image voltage-sensitive dye fluorescence in the supragranular layers with subcolumnar resolution. We therefore began functional VSD imaging using the fiber technology.

Fiber Imaging of Sensory Responses under Anesthesia Using Voltage-Sensitive Dye

To better understand the fluorescence signals imaged with the fiber, we compared the conventional epifluorescence tandem lens optics with the fiber optics. We imaged the whisker-evoked voltage-sensitive dye signals in the urethane anesthetized mouse barrel cortex using conventional optics and fiber optics in the same animal, using otherwise identical experimental conditions (Figure 3). In order to gain greater consistency from animal to animal, all our experiments were conducted on the signaling pathway that begins with one defined whisker. We chose to study the right C2 whisker, and all other whiskers on both sides were trimmed immediately before the experiment to a length of approximately 1 mm. Deflection of the C2 whisker excites sensory neurons of the trigeminal nerve, which signal primarily to the homologous region of the C2 barrel column of the somatosensory cortex via the brain stem and thalamus. To locate the C2 barrel column, we performed intrinsic optical imaging (Grinvald et al., 1986) through the intact skull (Figure 3A, left). A craniotomy centered on the C2 barrel column was then performed using the blood vessel pattern (Figure 3A, middle) for anatomical landmarks relative to the intrinsic signal. The blood vessels (aligned in serial tangential brain slices as they penetrate into the cortex) were also used in the post hoc alignment of cytochrome oxidase-stained tangential brain slices (Figure 3A, right), allowing the overlay of the barrel map (Figure 3D) on the functional images. RH1691 was applied to the craniotomy for an hour to evenly stain the cortex. A glass coverslip was placed in direct contact with the cortex to seal the craniotomy, which allowed the fiber to be repeatedly attached and removed from the animal in an easily reversible manner. The C2 whisker was deflected for 2 ms by a piezoelectric bimorph under computer control and the sensory response was observed in the barrel cortex after ~10 ms latency (Petersen et al. 2003a, Derdikman et al. 2003). The earliest sensory response was localized to the C2 barrel column, which was confirmed in three animals by cytochrome

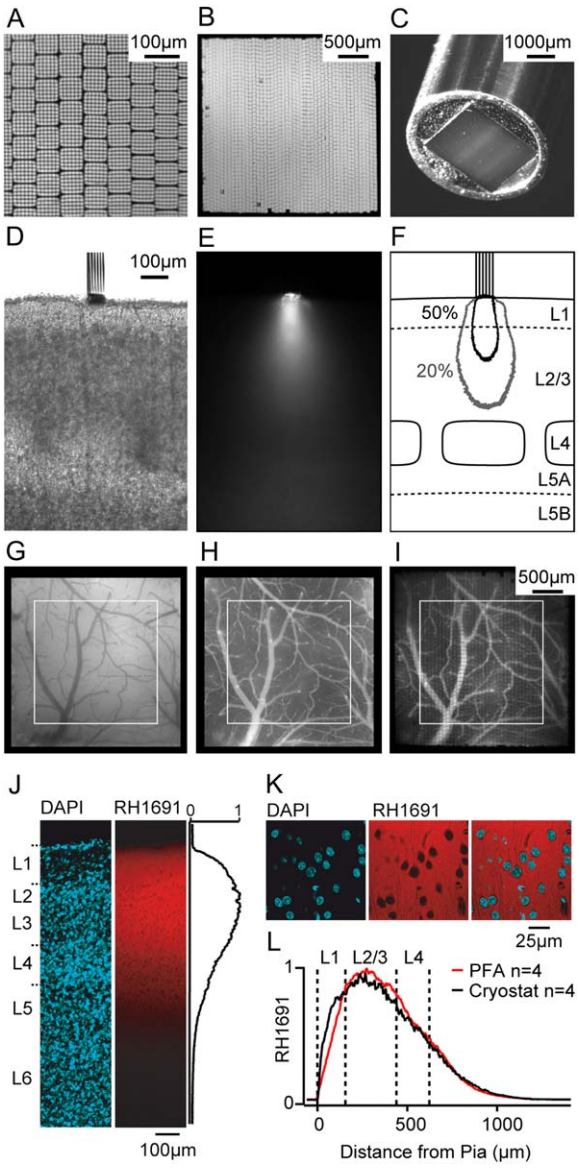

Figure 2. The Fiber Bundle Images Fluorescence in the Supragranular Cortex at Subcolumnar Resolution

(A) High-magnification micrograph of the end of the fiber optic image bundle showing the arrangement of individual fibers (8 μm cores; numerical aperture: 0.6). Multifibers containing 6 × 6 individual fibers were assembled together in a larger bundle.

(B) Micrograph showing the 3 × 3 mm final bundle containing 300 × 300 individual fibers.

(C) The tip of the fiber optic array was enclosed in a nonmagnetic metal (diameter: ~5 mm). The end of the fiber was placed in direct contact with the cortical surface.

(D) A single multifiber (composed of 6 × 6 individual fibers) was placed in direct contact with an in vitro brain slice of the mouse primary somatosensory barrel cortex.

(E) Excitation light (630 nm) was guided through the multifiber to analyze the penetration of light into the brain slice.

(F) Excitation light penetrated cortical layers 1, 2, and 3 with little reaching layer 4 or infragranular layers.

(G) Cortical surface blood vessels visualized with standard optics under green light (530 nm) illumination.

(H) Same cortical area imaged with standard epifluorescence optics after injection of the tail vein with ~100 μl of 1 mg/ml voltage-sensitive dye RH1691.

(I) Fluorescence of the blood vessels imaged via the fiber optic image bundle. Comparison of (G), (H), and (I) reveals that even small surface vessels were clearly visible with the fiber fluorescence imaging, attesting to a good horizontal spatial resolution. There is a slight reduction in image quality at the periphery of the fiber. All functional VSD imaging was therefore made within the central 2 × 2 mm region of the fiber indicated by the white square (also in [G] and [H]).

(J) After a functional VSD imaging session, the mouse brain was fixed with paraformaldehyde and cut in 100 μm thick parasagittal slices, which were counterstained with DAPI. Confocal images of these slices show that the RH1691 fluorescence was preferentially located in neocortical layer 2/3.

(K) Higher-magnification micrographs reveal that the dye was excluded from intracellular compartments.

(L) Average depth penetration of RH1691 measured from four mice with paraformaldehyde-fixed brains (PFA, red trace) and four mice with flash-frozen brains (cryostat, black trace) showing preferential labeling of layer 2/3.

oxidase staining of the layer 4 barrels followed by computer-aided alignment with the blood vessels. The response subsequently spread over the entire barrel cortex over the next 20 ms. Resonance vibrations of the piezoelectric bimorph wafers did not make a significant impact upon the cortical sensory responses, which were dominated by the brief high velocity onset whisker deflection (Figure S1). This pattern of sensory-evoked activity was imaged by both the conventional epifluorescence optics and the fiber optics (Figures 3B and 3C; Movie S2). We repeatedly switched back and forth between fiber and conventional optics three times in each experiment, and in all cases we observed similar spatiotemporal dynamics when comparing fiber and conventional optics. Quantification of the VSD signals showed that time course and amplitude of the signals recorded were almost identical between fiber and conventional optics (Figures 3E and 3F). This comparison was repeated in nine mice, and across these experiments we found that there was no difference between fiber and conventional optics in regards to the peak amplitude ($p = 0.94$), the duration (half-width, $p = 0.21$), or the spatial extent (the area responding with over half the peak amplitude, $p = 0.27$) of the sensory response (Figure 3G).

Voltage-Sensitive Dye Signals Correlate with Changes in Membrane Potential of Layer 2/3 Neurons

The fiber and the conventional optics report the same functional signals relating to voltage-sensitive dye RH1691, which is preferentially located in layer 2/3 (Figures 2J–2L). It is thus likely that the VSD signals would relate to membrane potential changes in layer 2/3. To directly test this, we performed whole-cell recordings from layer 2/3 neurons of the C2 cortical column while imaging VSD fluorescence under conventional optics in urethane anesthetized mice (n = 10 animals). As illustrated in Figures 4A–4C, the VSD signal quantified from the C2 column location was closely correlated with the spontaneous subthreshold membrane potential changes. However, when we observed action potentials (APs) in the whole-cell recording, these were not correlated with large VSD signals (Figure 4A). Closer analysis averaging many APs shows that action potentials observed in single cells make no impact on the VSD signal (Figure 4D). The temporal kinetics of RH1691 are sufficiently fast to record action potentials (T. Berger, A. Borgdorff, S. Crochet, S. Lefort, H-R. Lüscher, and C. Petersen, unpublished data), and if action potentials occurred with

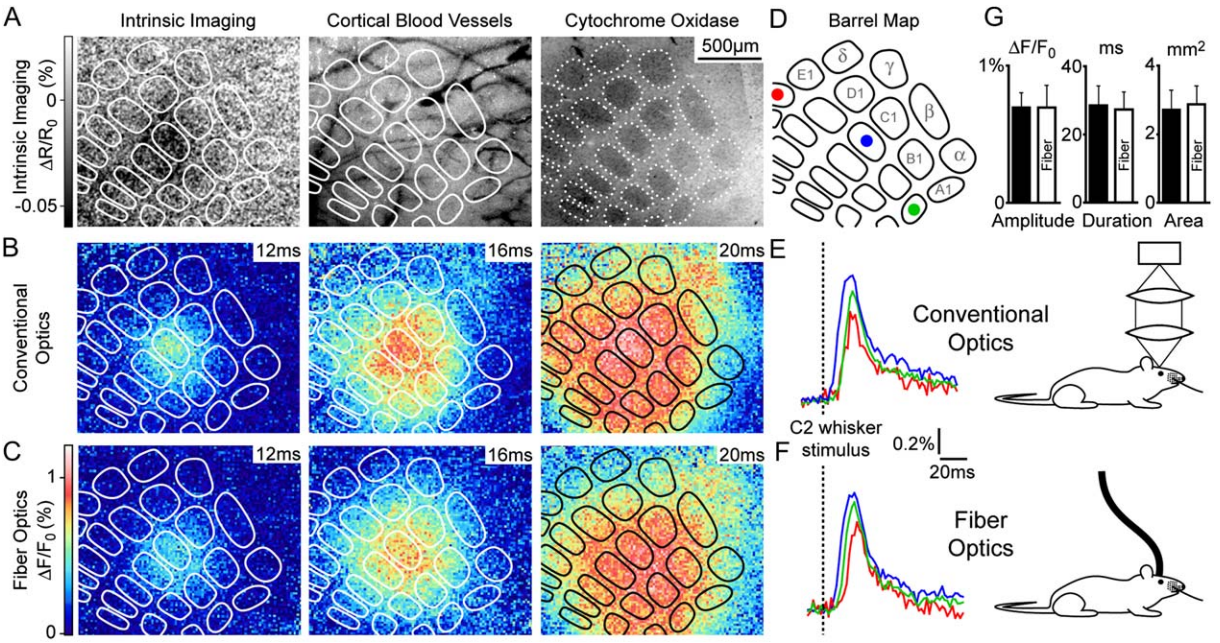

Figure 3. Fiber Optics and Conventional Optics Image Similar Voltage-Sensitive Dye Sensory Responses Evoked by Whisker Stimuli in Anesthetized Mice

(A) (Left) Intrinsic optical signal in response to repetitive C2 whisker stimulation (10 Hz, 4 s) imaged through the intact skull. This functionally identified location of the C2 whisker column was mapped onto the blood vessel pattern to guide surgery for the craniotomy. (Middle) Surface blood vessels visualized through the bone using 530 nm illumination. (Right) Cytochrome oxidase staining of layer 4 barrels. The VSD signals were aligned with the barrel map using the blood vessels.

(B) Voltage sensitive dye (RH1691) imaging of responses to single C2 whisker deflections (2 ms) observed using conventional epifluorescence optics (data averaged from n = 10 sweeps). The earliest response to the C2 whisker stimulation was localized to the C2 barrel column. Over the next tens of milliseconds depolarization spread to cover the entire barrel cortex.

(C) Imaging of responses to single C2 whisker deflections observed using the fiber optic image bundle (data averaged from n = 10 sweeps). The spatiotemporal dynamics of the sensory response recorded by the fiber bundle is similar to that observed with conventional optics.

(D–F) Quantification of VSD signals from ~100 × 100 μm areas centered on the E2 (red), C2 (blue), and A2 (green) barrel columns. Both time course and amplitude of the VSD signals were almost identical between fiber and conventional optics.

(G) Quantification of VSD signals imaged in response to C2 whisker stimulation with conventional optics and fiber optics across nine experiments. Response amplitude, duration (half-width), and spatial extent (area excited over half-maximal amplitude) showed no significant difference between conventional and fiber optics (p = 0.940, 0.205, and 0.274, respectively).

millisecond synchronization in a large fraction of the neuronal population, they would be observed in the VSD signal. The data thus suggest that spontaneous APs do not occur simultaneously in a large fraction of neurons. We therefore removed APs from the membrane potential traces by median filtering before computing the correlation of subthreshold membrane potential and VSD fluorescence. Across the ten experiments with simultaneous imaging and whole-cell recording, we obtained a Pearson's correlation coefficient of r = 0.68 ± 0.18 ($p < 0.001$) for spontaneous activity. The spontaneous depolarizations observed in whole-cell recordings corresponded to propagating waves of excitation as illustrated in Figure 4C. In each of these experiments, we also recorded VSD fluorescence and membrane potential changes evoked by C2 whisker deflections (Figures 4E–4G). The time course of the membrane potential changes during the cortical sensory response was very similar to the time course of the VSD signal. Plotting the VSD signal amplitude as a function of membrane potential also revealed a close to linear relationship between these two signals during evoked responses (Pearson's correlation coefficient r = 0.81 ± 0.18, n = 10, $p < 0.001$). Heartbeat-related artifacts were an order of magnitude smaller than the amplitude of the spontaneous waves, and there were no measurable breathing-related artifacts (Figure S2).

The VSD signals measured by conventional optics therefore correlate closely with the membrane potential changes of layer 2/3 neurons in the mouse barrel cortex (as observed in rat barrel cortex, Petersen et al., 2003a, 2003b). Since the VSD signals recorded by conventional optics match the signals recorded by the fiber optics, we can conclude that the fiber optics also image the membrane potential changes in layer 2/3.

Comparing Sensory Responses in Anesthetized and Awake Mice

We next asked how layer 2/3 cortical sensory responses might differ between anesthetized and awake animals. To investigate this we used isoflurane anesthesia, which offers both rapid induction and wake up, and in all experiments we repeatedly went in and out of anesthesia several times to validate the robustness of experimental findings. Reproducible whisker deflections in an awake, freely moving mouse were evoked by attaching a small metal particle to the C2 whisker and generating brief magnetic pulses (Figures 5A and 5B). Each single magnetic pulse reliably evoked a brief whisker movement as measured by an optical displacement sensor (Figure 5B).

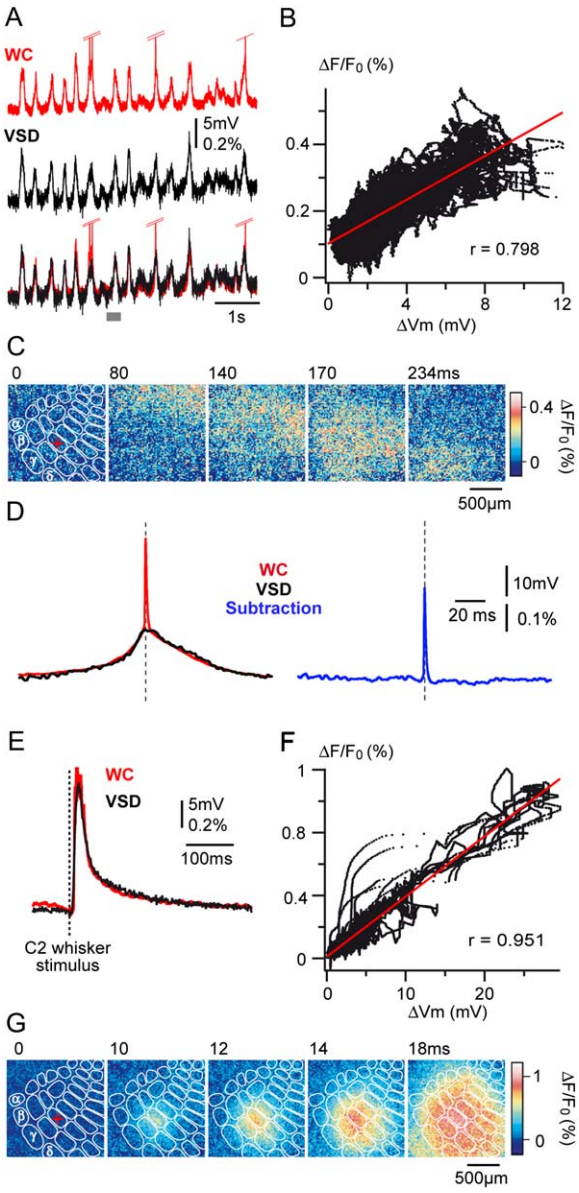

Figure 4. VSD Signals Correlate with the Membrane Potential of Layer 2/3 Neurons

(A) Whole-cell (WC) recording of a layer 2/3 neuron of the C2 cortical barrel column was performed simultaneously with measurement of VSD fluorescence under conventional optics in a urethane anesthetized mouse. Typical traces showing the WC recording (with truncated APs, red) and the VSD florescence (black) quantified from the C2 column location during spontaneous activity. The overlay of WC and VSD traces reveals a close correlation between the spontaneous subthreshold membrane potential and the VSD fluorescence changes. However, spontaneous APs were not correlated with large deflections of the VSD signal.

(B) The VSD signal plotted as a function of change in subthreshold membrane potential (Vm; APs were removed with a median filter) demonstrates a close to linear relationship.

(C) VSD images corresponding to a spontaneous depolarization recorded in WC (indicated by a gray bar in panel [A]). The red cross on the first image indicates the center of the region used to quantify the VSD fluorescence and the targeted location for the WC recording. These images show that the spontaneous depolarization recorded in WC corresponded to a propagating wave of excitation which crossed the entire barrel cortex.

(D) The VSD signal was aligned to APs recorded in the WC configuration and averaged across many APs (n = 29, from eight experiments). The subthreshold depolarization is nearly identical between the WC membrane potential recording and the VSD signal. However, the action potential is observed exclusively in the WC trace. The subtraction of the appropriately scaled traces (right) shows that the action potential is specifically missing from the VSD traces. This suggests that APs do not occur with millisecond synchronization in a large fraction of cortical neurons.

(E) For the same neuron, Vm changes in response to C2 whisker deflection were recorded while imaging VSD fluorescence. The averaged WC recording (red) and VSD signal measured from the C2 column location (black) are superimposed (n = 6 sweeps). The time course of the Vm changes during the cortical response to C2 whisker deflection was similar to the VSD signal.

(F) The VSD signal is plotted as a function of change in membrane potential for each individual sweep (APs were removed from Vm trace by a median filter). The two signals were linearly correlated.

(G) Image sequence corresponding to the average cortical responses shown in panel (E).

Fiber imaging of voltage-sensitive dye signals revealed that these stimuli evoked robust sensory responses in the barrel cortex of both anesthetized and awake mice (Figures 5C and 5D). Qualitatively, many aspects of the sensory responses were similar between anesthetized and awake conditions (as also suggested by Chapin and Lin, 1984). The magnetic deflection of the C2 whisker evoked a sensory response that began in the C2 barrel column and spread over a large area of the barrel cortex. The duration of the sensory response was significantly longer in awake animals (half-width: 86 ± 69 ms), than in animals under isoflurane (37 ± 8 ms, $p = 0.016$), likely reflecting more complex processing of the sensory signals (Krupa et al., 2004) in an awake mouse (Figures 5C–5E). The area responding with over half the peak amplitude of the sensory response also increased significantly in awake animals (2.87 ± 0.51 mm^2) compared to anesthetized mice (1.66 ± 0.81 mm^2; $p < 0.001$). This suggests that the surprisingly large area of cortex that can be excited by a single whisker stimulus is not an artifact of anesthesia, but is an important integrative property of sensory processing also occurring in awake animals. Quantitatively, the peak amplitude of the sensory response in awake animals (0.33% ± 0.20%) on average was larger than that of animals under isoflurane anesthesia (0.26% ± 0.11%), although not significantly ($p = 0.35$). The lack of significance likely reflects the very high variability of the sensory response during the awake recordings (Figure 5E). When we quantified whisker-related behavior, we found that a large part of this response variability can be accounted for by differences in ongoing behavior at the time of stimulus delivery.

Sensory Responses during Quiet and Active Whisker Behavior

We combined the functional VSD imaging of somatosensory barrel cortex with high-speed filming of the mouse behavior with particular attention paid to obtaining high-contrast images of the C2 whisker. The behavioral platform was illuminated from below with infrared light from a custom-made LED array. The silhouette of the mouse and its whiskers were filmed using a high speed camera allowing up to 2 ms temporal resolution and a spatial resolution of 0.2 mm with a field of view of 20 × 20 cm. We tracked the position of the head, the head direction and the C2 whisker angle (Figure S3; Movie S3) for each frame of the recorded movies, either

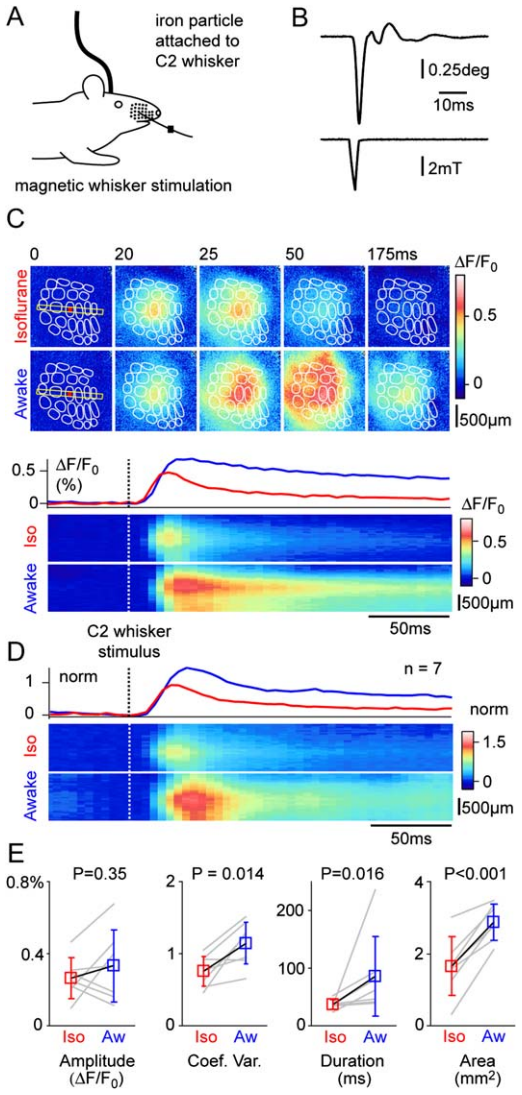

Figure 5. Evoked Sensory Responses Last Longer and Spread Further in Awake Compared to Anesthetized Mice

(A) To evoke reproducible whisker stimuli in freely moving mice, a small metal particle was attached to the C2 whisker and brief magnetic pulses (1–5 ms) were delivered through an electromagnetic coil.

(B) The whisker displacement induced by the magnetic pulse was measured with an optical displacement sensor (upper trace). The magnetic field was also measured (lower trace) and we verified that each single magnetic pulse reliably evoked whisker displacement. The magnetic field was uniform across the entire xy plane of the behavior platform that was placed in the center of the magnetic coil.

(C) Comparison of cortical responses to C2 whisker deflections imaged by VSD in a mouse while it was either under isoflurane anesthesia or awake. Averaged data from 30 sweeps are shown for each condition. The time course of the VSD signal quantified from the C2 barrel column (region shown in red on the first image of the image sequences) reveals that the duration of the response was much longer when the mouse was awake (middle panel). Linescan plot (time on x axis and space on y axis) of the VSD signal from a region crossing the barrel cortex (yellow rectangle on the first image of the image sequences) is shown in the lower panel.

(D) VSD responses to C2 whisker deflection were compared between isoflurane anesthesia and wakefulness in seven animals. Responses were normalized to the amplitude evoked during isoflurane anesthesia and averaged.

(E) The peak amplitude of the sensory response in awake animals on average was larger than under isoflurane anesthesia (although not significantly). The coefficient of variation, the duration and the spread of the sensory response were significantly larger in awake animals.

by hand or by automated image analysis (L. Segapelli, S. Crochet, I.F., C.P., D. Sage, and M. Unser, unpublished data). We then studied how sensory responses evoked by delivering magnetic whisker-stimuli in freely moving animals differed during active whisking compared to periods when the animal was quiet. In addition to this detailed behavioral analysis, we also measured the EEG in three additional mice, finding consistent changes in the power spectrum differentiating between isoflurane anesthesia, sleep, quiet wakefulness, and whisking (Figure S4). When the mouse was still and not whisking, passive magnetic deflection of the C2 whisker could evoke large sensory responses, which propagated across the barrel cortex. The sequence of events in the experiment shown in Figures 6A and 6B and in Movie S4 is particularly interesting. At the beginning of the sequence the animal is quiet and the whiskers are not moving. The magnetic stimulus evokes a small whisker deflection in the z direction, which is normal to the plane of the behavioral imaging and therefore not recorded on the plot of whisker position. The sensory response begins ~10 ms after whisker deflection in a localized region of the C2 barrel column and then spreads across the barrel field. Approximately 70 ms after the peak of the sensory response, the mouse makes an active whisker movement, protracting its whisker a long way forward. We think this active whisker movement resulted from the mouse perceiving the applied sensory stimulus and then proceeding to actively investigate the cause of the whisker deflection. Equally, one can speculate that the wave of excitation that we observed propagating across the barrel cortex is only the beginning of a more complex wave of excitation encompassing larger brain areas and perhaps exciting the motor cortex to drive whisker movement. The very next stimulus in this experiment was delivered some minutes later when the animal was actively whisking (Figures 6C and 6D; Movie S5). In this case, only a small sensory response evoked by the passive magnetic stimulus was observed in the barrel cortex during whisking, and there were no obvious alterations in behavior (Figures 6C and 6D; Movie S5). This reduction in the amplitude of the passively evoked sensory response during active whisking was extremely robust and accounted for a large part of the variability of the sensory responses in awake mice. The peak amplitude of sensory responses in the C2 barrel column was quantified for each individual sweep and categorized according to the whisker-related behavior at the time of the stimulus. The mean amplitude of the sensory response during active whisking was reduced to 26.3% ± 16.8% (n = 6 mice, $p < 0.001$) of the quiet response. The enhanced responses during quiet behavior were observed in all six mice of this experimental series (Figures 6E and 6F).

Imaging Spontaneous Waves during Quiet Behavior

In addition to the large sensory responses observed during quiet behavioral periods, we also observed spontaneous waves of activity, which propagated across the imaged area of the barrel cortex in freely moving mice when they were not actively exploring their environment (Figure 7; Movie S6). The direction of the waves was

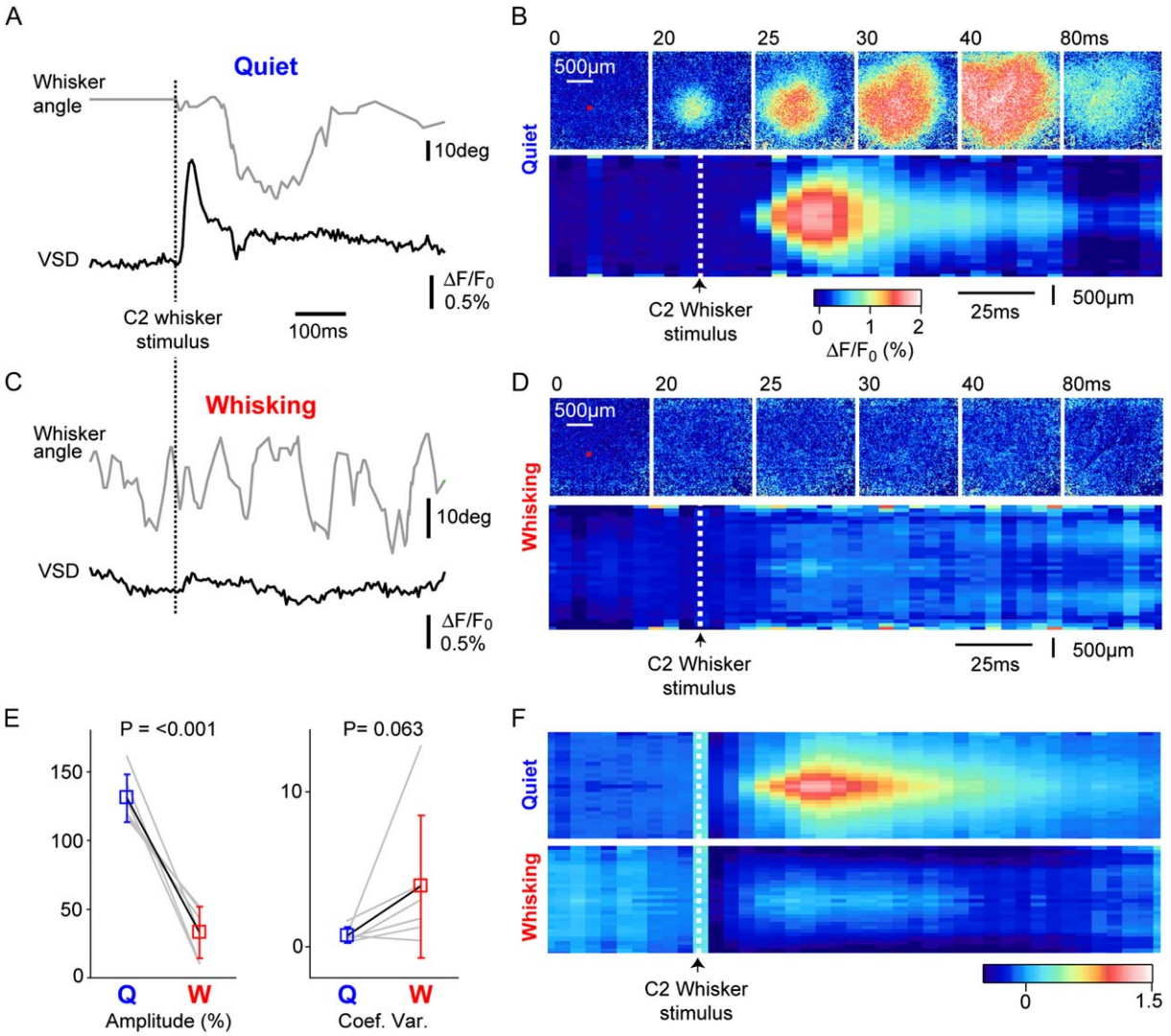

Figure 6. The Evoked Sensory Response in Freely Moving Mice Depends Strongly on Behavior

(A) Example of a sensory response to C2 whisker deflection imaged with VSD while the mouse was sitting still and not whisking (as indicated by the prestimulus whisker angle, gray trace). As the displacement of the whisker induced by the magnetic pulse was in the vertical direction, it does not appear on the whisker angle trace, which plots only the horizontal whisker position. The VSD signal (black trace) quantified from the center of the C2 column (red square on the first image in [B]) showed a large amplitude response following the stimulus. Note that approximately 70 ms after this cortical response, the mouse protracted its whisker as if to investigate what caused the whisker deflection.

(B) Image sequence corresponding to the cortical response shown in (A) (upper panel). The response was first restricted to a localized region and then spread across the barrel cortex. The outward radial spread of the VSD signal from the center of the response is shown in the lower panel (time is plotted on the x axis and space on the y axis).

(C) During the next sweep in the same experiment, the C2 whisker deflection occurred while the same mouse was actively whisking. Only a very small sensory response was observed in the VSD images.

(D) Image sequence and quantification of the VSD signal from the response shown in (C).

(E) The peak amplitude of sensory responses in the C2 barrel column was quantified for each individual sweep and categorized according to the whisker-related behavior at the time of the stimulus (quiet or whisking). VSD response amplitudes were normalized to the average evoked response for each experiment (n = 6). During quiet behavior the response amplitude was larger than average, whereas it was strongly reduced during whisking. Evoked responses may also be more variable during whisking than during quiet behavior, as suggested by the coefficients of variation.

(F) The outward radial spread of the VSD signals from the C2 barrel column compared between quiet and whisking behavior normalized across all six experiments.

different from one spontaneous event to the next. The velocity of the propagating wave-front was measured (Figures 7E and 7F) at the half-maximal amplitude and found to be highly variable. Interestingly, both the amplitude and velocity of the spontaneous waves were the same during quiet wakefulness as observed during urethane anesthesia (Figure 7F). The waves observed during urethane anesthesia correlate with UP and DOWN states (Petersen et al., 2003b), and their appearance during quiet wakefulness suggests that UP and DOWN states may also be a feature of some awake states in mice.

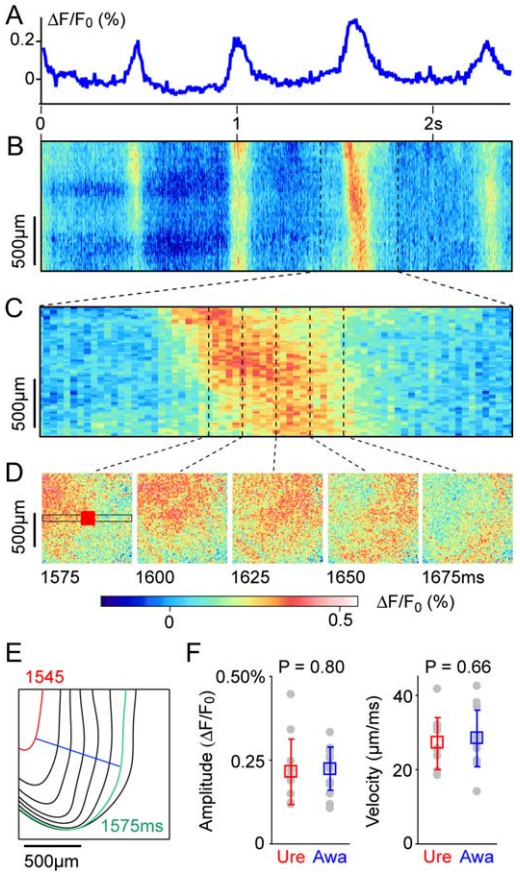

Figure 7. Spontaneous Waves of Cortical Activity Occur during Quiet Wakefulness

(A) VSD signal (quantified from the region indicated by the red square in panel [D]) reveals slow spontaneous depolarizations during quiet behavior.

(B) Linescan plot (time on x axis and space on y axis) of the VSD signal from a region crossing the barrel cortex (black rectangle in panel [D]) shows that these slow depolarizations crossed the entire barrel cortex.

(C) Temporal zoom of the plot in panel (B) showing that these slow depolarizations can occur as propagating waves of excitation.

(D) A time series of VSD images showing the propagating wave highlighted in panel (C).

(E) Wave-fronts corresponding to half-maximal amplitudes were computed from Gaussian-filtered VSD image sequences, in order to calculate the propagation velocity of the spontaneous events. Each contour is therefore derived from a different image occurring at a different time during the wave propagation. The velocity was taken as the maximal distance propagated by the half-maximal wave-front during a 30 ms interval (indicated by the blue line connecting two contours 30 ms apart).

(F) The amplitude and velocity of the spontaneous waves were computed from the awake mice and compared to spontaneous events recorded under urethane anesthesia. The quantitation revealed that these properties were remarkably similar between quiet wakefulness (n = 14 waves from three mice) and anesthesia (n = 11 waves from three mice).

We furthermore investigated whether we could observe patterns of activity in the primary somatosensory cortex that correlated with active whisking. Even after averaging many whisking cycles, only small-amplitude signals were detected, suggesting weak correlation between the ensemble average supragranular membrane potential and whisker movement. This surprisingly weak correlation may result from the activity of different individual neurons being tuned to different phases of the whisker cycle (Fee et al., 1997; Crochet and Petersen, 2006). The correlation would likely increase if the mice were trained to perform goal-directed whisking (Ganguly and Kleinfeld, 2004).

Imaging the Cortical Representation of Active Whisker Touch

We were concerned by the data suggesting that whisker stimuli evoked small sensory responses during active whisking. This is odd since it is thought that this is when the animal is actively gathering whisker-related information. It therefore seems that this should be the period in which whisker input should be particularly important for the mouse, and naively, one might then have expected larger sensory responses. We therefore performed experiments to investigate if there was sensory activity in the primary somatosensory barrel cortex when a mouse was actively exploring its environment and touched an object with its C2 whisker. We imaged mouse behavior and barrel cortex activity with the fiber optics as before, but now instead of applying passive stimuli to the whiskers with the magnetic stimuli, we allowed the mouse to touch objects placed in the behavioral chamber (Figure 8; Movie S7). We analyzed 11 whisker contacts which evoked VSD signals in three different animals. Whisker contact with an object was visualized with the high-speed camera and defined to occur at the first frame where the whisker was bent by the object contact (Figure 8). Although the amplitudes of cortical responses were highly variable (Figures 8C and 8E), the spatiotemporal dynamics of the recorded signals induced by active touches shared similar properties. The earliest cortical activity imaged immediately after C2 whisker contact occurred in a small localized region, from which it spread over a large part of the barrel cortex (Figure 8A). The location of the early response to active touch was found to be identical to the location of the early response evoked by passive whisker stimulation of the C2 whisker during anesthesia (Figure 8D). The sensory response during active touch with the C2 whisker therefore initiates in the C2 barrel column and the sensory information is distributed rapidly across the barrel cortex, allowing integration with multiwhisker input.

These images of active sensory processing in an awake, freely moving animal show that some aspects of the sensory processing of active touch appear similar to the sensory responses evoked by a passive stimulus (Figure 8B). The early signals are localized to the C2 whisker barrel column and spread over large cortical areas. The large cortical area excited by single whisker touch suggests that a single whisker can inform a large area of the brain under physiological conditions of recording in an awake, freely moving mouse.

Discussion

Whisker Sensation

Processing of single whisker-related information occurs through a similar spatiotemporal dynamic in anesthetized and awake animals. The earliest cortical supragranular responses occurred ~10 ms after whisker deflection and were localized to the isomorphic whisker barrel

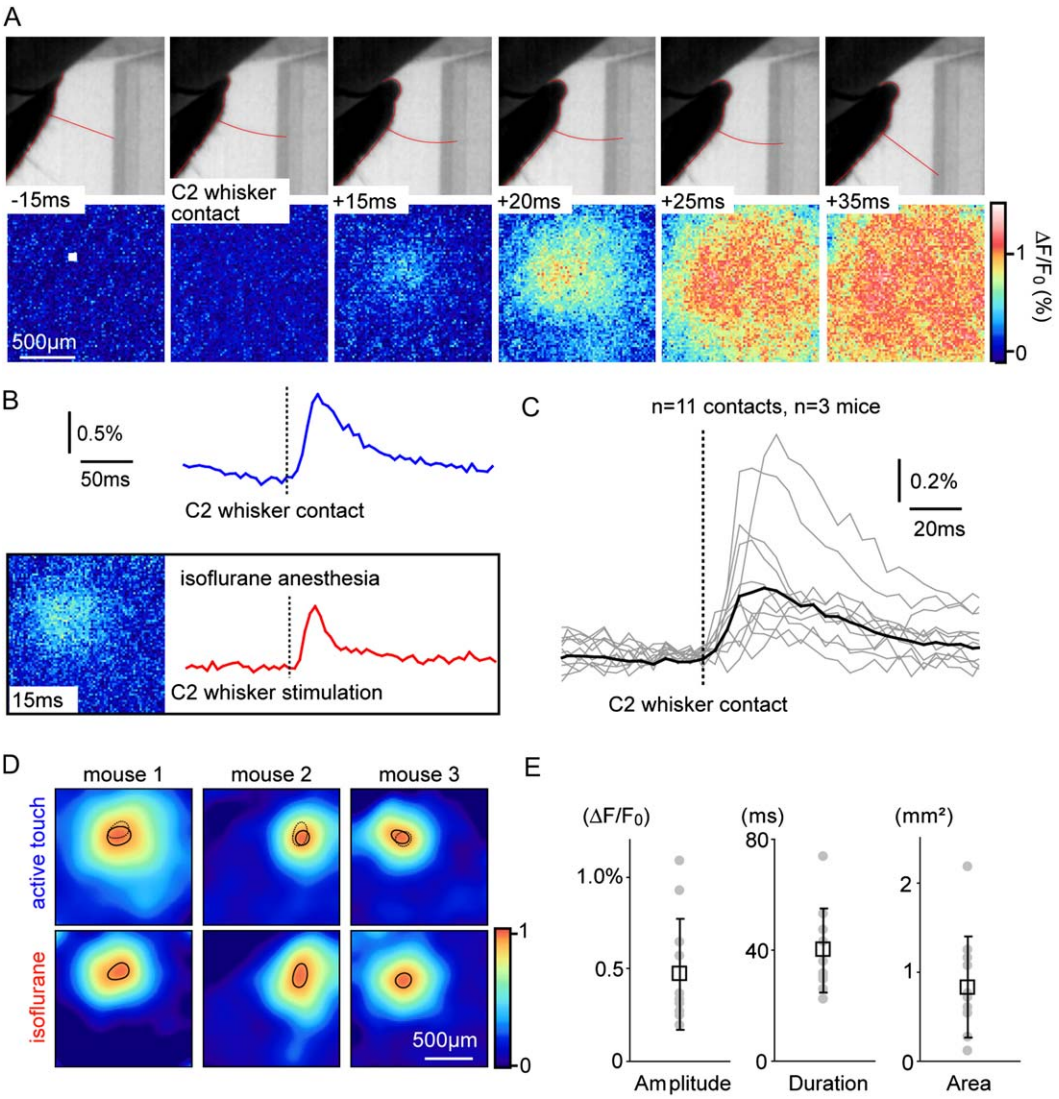

Figure 8. Imaging the Cortical Representation of Active Whisker Touch

(A) Images of the mouse behavior (upper panel) and the VSD signals from its somatosensory barrel cortex (lower panel) recorded as the mouse was approaching and actively touching an object with its C2 whisker. Active whisker touch evoked an initially localized sensory response, which over the next 20 ms propagated across the barrel cortex.

(B) VSD signal quantified from the region indicated by the white square in (A). The C2 whisker contact is followed by a large amplitude response. The image and trace in the box below show the VSD response to a passive C2 whisker deflection recorded while the mouse was under isoflurane anesthesia.

(C) VSD responses to 11 whisker contacts recorded in three mice. In each case the active whisker contact with an object evoked a brief propagating sensory response.

(D) The location of the early sensory response evoked by active touch is compared to the location of the early sensory response evoked by a piezo whisker stimulus under isoflurane anesthesia. The solid contour indicates the 95% contour of the evoked VSD response in each condition. In the active touch condition, the dotted contour indicates the location of the early sensory response evoked during isoflurane. There is excellent agreement of the location of the early sensory response in each of the three mice.

(E) The amplitude, duration (half-width), and spatial extent (area at half-maximal amplitude) were computed for each active contact.

column. The brain may compute which whisker was deflected by this early localized response (Petersen et al., 2001). Over the next tens of milliseconds depolarization propagated to cover the entire barrel cortex. This later spreading sensory response informs the neighboring cortical columns of the single whisker deflection and may underlie sensory integration of multiwhisker inputs. The distributed coding of single whisker deflection in layer 2/3 across the barrel cortex, which we visualized with voltage-sensitive dye, is also reflected in broad subthreshold receptive fields (Zhu and Connors, 1999; Moore and Nelson, 1998; Brecht et al., 2003). Interestingly, the subthreshold supragranular cortical dynamics of active touch (Figure 8) do not appear to be qualitatively different from passively evoked sensory responses. Indeed, responses to active touches consisted of early localized excitations that subsequently propagated across the barrel cortex. This spreading sensory response is likely to be mediated at least in part through the extensive lateral axonal arborizations of layer 2/3 pyramidal

neurons, which have been characterized previously (Keller and Carlson, 1999; Petersen et al., 2003a). The propagating sensory response is therefore a physiological signature of single whisker deflection, but during natural tactile processing animals use the entire array of whiskers. During object palpation many whiskers would near-simultaneously make contact, and it is therefore important to note that previous observations have highlighted profound roles for suppression of principal whisker responses by neighboring whiskers (Simons, 1985; Kelly et al., 1999; Higley and Contreras, 2005). In addition, sensory experience plays a profound role in regulating the receptive-field properties of barrel cortex neurons (recently reviewed by Feldman and Brecht, 2005), resulting in changes in the map representation of individual whiskers (Polley et al., 1999, 2004). It will therefore be of great interest in future studies to image cortical sensory processing during active touch of objects with the complete array of whiskers in mice, with different histories of sensory experience and during learning.

It seems counterintuitive that smaller sensory responses to passive magnetic whisker stimulation are evoked during active whisking behavior, since this is when one might expect whisker-related sensory processing to be most relevant for the animal. However, the suppression of sensory responses during active behavior (an issue first raised by Chapin and Woodward, 1982) has also been observed in whole-cell recordings (Crochet and Petersen, 2006), extracellular unit activity (Fanselow and Nicolelis, 1999; Hentschke et al., 2005), and field potential recordings (Castro-Alamancos, 2004; Hentschke et al., 2005). In our experiments, the magnetic field, and hence the force applied to the whisker, was consistent between quiet and active periods, but we do not know if the same activity was evoked in the trigeminal nerve. However, previous studies found that sensory responses evoked by direct stimulation of the sensory nerve were also suppressed during whisking (Fanselow and Nicolelis, 1999; Castro-Alamancos, 2004; Hentschke et al., 2005). The suppression of the sensory response during whisking is therefore, at least in part, mediated by processes downstream of the whisker follicle. One possible contribution to the suppression is that thalamic synapses may be weakened during whisking by short-term synaptic depression induced by increased thalamic "background" firing rates (Chung et al., 2002; Castro-Alamancos and Oldford, 2002). Another likely contribution to sensory response suppression is that the cortical brain state is different between quiet and whisking behavior (for example, spontaneous waves of activity were only observed during quiet periods and the EEG spectra are different), and this could affect how synaptic inputs are integrated in the context of ongoing spontaneous activity.

Having found strongly depressed sensory responses during active whisking, it is then a surprise that we were able to record sensory responses during active touch. The trigeminal sensory neurons may be engaged in a different manner during active touch as compared to passive stimuli (Szwed et al., 2003). During active whisking, vibrissae may be actively accelerated into objects by a recently described early feedback motor loop in the brainstem (Nguyen and Kleinfeld, 2005). Sensory activity in the trigeminal neurons generated by an initial object contact would be amplified as the whisker was accelerated into the object, driving increasing deflection of the whisker. However, if the sensory stimulus is not attributed to a physical object, then the whisker acceleration will only pass through air and it will thus have less consequence. This positive feedback loop would therefore specifically amplify activity in sensory neurons when the whisker contacted a real object.

In addition, there may be "top-down" influences on the sensory activity of the barrel cortex. As the mouse explores its environment, it is likely to construct a mental image of its environment. Because it moves the whisker through a given region of space many times, it may interpret our passive magnetic stimulus as just noise—it has already had the whisker through that region of space and on previous whisks it did not contact an object. It may be that our passive whisker stimulus is then actively filtered out as noise.

The variability of the cortical processing of whisker sensation that we have observed may correlate with different perceptual thresholds. To investigate this, we are now beginning to train mice to perform sensory discrimination linked with specific motor output to inform us of the mouse percept. It will then be interesting to see if the smaller sensory responses evoked during whisking correlate with reduced perception.

Applications and Technological Outlook

A major advantage of the current fiber-based imaging technique that we describe here is that it is relatively simple and easy to use, in contrast to the advanced technology of the head-mounted, scanning, two-photon fiber imaging system that has been recently developed (Helmchen et al., 2001). It should therefore be easy to transfer the technique to make measurements of other sensory areas. Of particular interest to us would be the simultaneous imaging of both primary and secondary somatosensory cortices. Equally, it should be straightforward to apply the current fiber-based imaging technique for measurements of visual cortex, motor cortex, and the olfactory bulb in freely moving animals. Ideally, one might be able to image simultaneously from the entire dorsal aspect of the neocortex; this could be achieved by shaping the fiber end so that it envelopes the whole cortex.

We think the most important technical advances that need to be made for this fiber imaging technology will be those that allow repeated imaging from trained animals. Repeated voltage-sensitive dye imaging has been achieved in monkeys (Slovin et al., 2002) through the development of artificial dura. For rodents, implanted canula to deliver the dye within a sealed imaging window over a craniotomy (Holtmaat et al., 2005) are likely to offer the best possibilities. Recent advances in developing genetically encoded fluorescing membrane potential sensors (Siegel and Isacoff, 1997; Cacciatore et al., 1999; Sakai et al., 2001; Ataka and Pieribone, 2002) may help long-term chronic imaging and in addition could offer cell type-specific labeling.

In conclusion, there are many further applications and future developments to be made based on fiber imaging. Here, we have demonstrated that fiber bundle-based, voltage-sensitive dye imaging is useful for analyzing the dynamics of cortical function in freely moving mice,

allowing a correlation of brain function and behavior on a millisecond timescale with subcolumnar resolution.

Experimental Procedures

Animals and Surgery

All experiments were carried out in accordance with authorizations approved by the Swiss Federal Veterinary Office. C57BL6J mice aged 1 to 5 months were anesthetized with either urethane (1.5 mg/g) or isoflurane (1.5%). Paw withdrawal, whisker movement, and eyeblink reflexes were largely suppressed. A heating blanket maintained the rectally measured body temperature at 37ºC. The head of the mouse was fixed by a nose clamp. The skin overlying the somatosensory cortex was removed and the bone gently cleaned.

Intrinsic Optical Imaging

The cortical surface was visualized through the intact bone covered with Ringer's solution and sealed with a glass coverslip. The surface blood vessels were visualized using light of 530 nm to enhance contrast. The illumination was switched to 630 nm for functional imaging. The reflected light was imaged using a Qicam CCD camera (Q-imaging) coupled to a Leica MZ9.5 microscope. Image acquisition via FireWire and stimulus control via an ITC-18 (Instrutech) was governed by custom routines running in IgorPro (Wavemetrics). Alternating sweeps were imaged with or without piezo stimuli delivered to the C2 whisker. Stimuli were applied at 10 Hz for 4 s and the intrinsic signal was quantified as the difference in the reflected light upon stimulus compared to immediately before. The intrinsic imaging gave a localized signal centered on the C2 barrel column. This functionally identified location of the C2 barrel column was mapped onto the blood vessel pattern to guide surgery for the craniotomy.

Voltage-Sensitive Dye Imaging

A 2 × 2 mm craniotomy was made, centered on the location of the C2 barrel column as determined by the intrinsic optical imaging. Extreme care was taken at all times not to damage the cortex, especially during the removal of the dura. Voltage-sensitive dye RH1691 was dissolved at 1 mg/ml in Ringer's solution containing the following (in mM): 135 NaCl, 5 KCl, 5 HEPES, 1.8 $CaCl_2$, and 1 $MgCl_2$. This dye solution was topically applied to the exposed cortex and allowed to diffuse into the cortex over 1 hr. The cortex was subsequently washed to remove unbound dye.

In experiments where conventional epifluorescence imaging was compared to fiber imaging, the cortex was then sealed by gluing on a glass coverslip which was in direct contact with the cortical surface. In experiments combined with electrophysiology, the cortex was covered with agarose and a coverslip placed on top in a manner that allowed access for recording pipettes. In all experiments performed with urethane anesthetized mice, electrocardiogram (ECG) electrodes were inserted under the skin of the forearms.

In the fiber imaging experiments, a U-shaped aluminum fiber holder was first implanted, centered on the location of the C2 barrel column, before performing the craniotomy and dye staining. The fiber holder was designed to allow reproducible placement and orientation of the fiber. During epifluorescent visualization, the fiber tip was placed in direct contact with the cortical surface, and fixed in place to the fiber holder using dental cement.

The voltage-sensitive dye was excited with 630 nm light from a 100 W halogen lamp gated by a Uniblitz shutter (Vincent Associates) under computer control via an ITC-18 (Instrutech) communicating with custom software running within IgorPro (Wavemetrics). The excitation light was reflected using a 650 nm dichroic and focused onto the cortical surface or the proximal fiber end with a 25 mm video lens (Navitar). Fluorescence was collected via the same optical pathway, but without reflection of the dichroic, long-pass filtered 665 nm, and focused onto the sensor of a high-speed MiCam Ultima (Scimedia) camera via a 135 mm camera lens (Nikon).

Fiber Optics

The fiber optics were custom made by Schott Fiber Optics based on their wound image bundle technology (http://www.schott.com/fiberoptics).

Whole-Cell Recordings

Pipettes were slowly advanced into the cortex under high positive pressure (~200 mbar) and targeted to the functionally mapped C2 barrel column. Positive pressure was reduced (~25 mbar) and the pipette was advanced in 2 μm steps until the pipette resistance increased, and then suction was applied to establish a gigaseal followed by the whole-cell configuration. Whole-cell pipettes had resistances of ~5 MΩ filled with a solution containing the following (in mM): 135 potassium gluconate, 4 KCl, 10 HEPES, 10 phosphocreatine, 4 MgATP, 0.3 Na_3GTP (adjusted to pH 7.2 with KOH), and 2 mg/ml biocytin. Whole-cell electrophysiological measurements were made with a Multiclamp 700 amplifier (Axon Instruments). The membrane potential was filtered at 10 kHz and digitized at 20 kHz in a sweep-based manner by an ITC-18 (Instrutech Corporation) under the control of IgorPro (Wavemetrics).

Whisker Stimuli

For the experiments performed with anesthetized mice, 2 ms C2 whisker deflections were generated by using a computer-controlled piezoelectric bimorph. For the experiments performed with awake, freely moving mice, reproducible whisker deflections were evoked by attaching a small metal particle to the C2 whisker and generating brief magnetic pulses. Magnetic pulses were generated by a copper wire coil with 1500 windings totaling 50 cm height in the z direction and 20 cm diameter in the xy plane. Single brief current pulses (1–5 ms) were driven through the coil by discharge from a capacitor gated by a solid-state relay under computer control. The magnetic field was measured at different positions within the coil and was found to be uniform across the entire xy plane in the central 20 cm of the z direction. The behavioral platform, where the mouse was placed, was therefore mounted in this central z location.

Filming and Quantifying Whisker Behavior

The behavioral area was illuminated from below with infrared light and filmed through a 50 mm video lens (Navitar) with a high-speed MotionPro camera (Redlake). This transillumination gave a high contrast silhouette of the mouse body and sufficient contrast to visualize the mouse whiskers. The field of view was 20 × 20 cm, giving a single pixel resolution of 0.2 mm. The behavioral images were obtained at either 2 ms or 5 ms intervals between frames and imaging was synchronized to the voltage-sensitive dye imaging through TTL pulses. Custom-written routines running within ImageJ were used to automatically track head and whisker position (L. Segapelli, S. Crochet, I.F., C.P., D. Sage, and M. Unser, unpublished data).

Analysis of Voltage-Sensitive Dye Images

VSD image sequences acquired with the high-speed MiCam Ultima camera were analyzed using custom-written routines in IgorPro (Wavemetrics).

In all experiments performed with urethane anesthetized mice, alternating sweeps triggered on a fixed phase of the ECG were imaged with or without stimuli delivered to the C2 whisker. Subtraction of the averaged unstimulated sweeps was then used to correct both bleaching and heartbeat-related artifacts. In experiments combined with electrophysiology, image sequences of spontaneous cortical activity were corrected for bleaching by subtracting the exponential fit of the average fluorescence decrease over the time. For all the experiments performed with awake, freely moving mice, the ECG was not monitored. Therefore, VSD signals were not corrected for heartbeat artifacts, but bleaching was corrected for by linear fits to the average fluorescence decay. In experiments where sensory responses in anesthetized mice were compared to responses in awake mice, alternating sweeps with or without stimuli delivered to the C2 whisker were recorded. Subtraction of the averaged unstimulated sweeps was then used to correct for bleaching.

Recordings of VSD signals presented surprisingly small heartbeat-related artifacts (Figure S2). However, large movements of the mice, such as jumping or running into the wall of the behavioral chamber, were accompanied with movement-related artifacts. These movement-related artifacts could be clearly differentiated from VSD signals reflecting neuronal activity since (1) they were correlated across the entire imaged area, (2) they occurred in cortical areas not stained with VSD, and (3) the movement artifacts were highlighted at the border of the craniotomy.

VSD signals were quantified as the mean pixel value within square regions of interest. Linescan plots were calculated by averaging pixel values along short segments in the normal direction to a defined line crossing the barrel cortex. Outward radial spread plots were calculated by averaging pixel values from circular regions of interest (rings) of increasing diameter around a given center location.

Histology

After completion of the physiological measurements, mice were deeply anesthetized with urethane and perfused with PBS followed by 4% paraformaldehyde. After fixation, 100 μm thick brain slices were cut. Most brains were sectioned tangentially, stained for cytochrome oxidase revealing the layer 4 barrel map, and the VSD signals aligned using the blood vessels. Other brains were sectioned parasagitally to analyze the penetration and staining of voltage-sensitive dye RH1691 by confocal microscopy (Leica SP2). In four additional experiments, the mouse brain was rapidly frozen in isopentane chilled by dry ice, transferred to a cryostat (Leica CM3050S), and sectioned in 20 μm thick parasagital slices.

Statistical Tests

Data are expressed as mean ± standard deviation, and they were tested using SigmaStat (Systat Software) for statistical significance using Student's t test (paired when appropriate) or Wilcoxon signed rank test (for data without a normal distribution).

Supplemental Data

The Supplemental Data for this article can be found online at http://www.neuron.org/cgi/content/full/50/4/617/DC1/.

Acknowledgments

The authors are grateful for the generous support of the Swiss National Science Foundation and the Leenaards Foundation. We thank Amiram Grinvald and Bert Sakmann for help and advice concerning voltage-sensitive dye imaging. We thank Mathew Diamond and Ehud Ahissar for help and advice on how to obtain high-contrast filming of whiskers. We thank Rolf Rödel (MPI Heidelberg) and Cedric Nicolas (EPFL) for electronic design and construction of the magnetic whisker stimulators. We thank Sylvain Crochet and James Poulet for discussion and critical reading of the manuscript.

Received: September 26, 2005
Revised: February 10, 2006
Accepted: March 28, 2006
Published: May 17, 2006

References

Arieli, A., Sterkin, A., Grinvald, A., and Aertsen, A. (1996). Dynamics of ongoing activity: explanation of the large variability in evoked cortical responses. Science *273*, 1868–1871.

Ataka, K., and Pieribone, V.A. (2002). A genetically targetable fluorescent probe of channel gating with rapid kinetics. Biophys. J. *82*, 509–516.

Brecht, M., Roth, A., and Sakmann, B. (2003). Dynamic receptive fields of reconstructed pyramidal cells in layers 3 and 2 of rat somatosensory barrel cortex. J. Physiol. *553*, 243–265.

Cacciatore, T.W., Brodfuehrer, P.D., Gonzalez, J.E., Jiang, T., Adams, S.R., Tsien, R.Y., Kristan, W.B., and Kleinfeld, D. (1999). Identification of neural circuits by imaging coherent electrical activity with FRET-based dyes. Neuron *23*, 449–459.

Castro-Alamancos, M.A., and Oldford, E. (2002). Cortical sensory suppression during arousal is due to the activity-dependent depression of thalamocortical synapses. J. Physiol. *541*, 319–331.

Castro-Alamancos, M.A. (2004). Absence of rapid sensory adaptation in neocortex during information processing states. Neuron *41*, 455–464.

Chapin, J.K., and Woodward, D.J. (1982). Somatic sensory transmission to the cortex during movement: gating of single cell responses to touch. Exp. Neurol. *78*, 654–669.

Chapin, J.K., and Lin, C.S. (1984). Mapping the body representation in the SI cortex of anesthetized and awake rats. J. Comp. Neurol. *229*, 199–213.

Chung, S., Li, X., and Nelson, S.B. (2002). Short-term depression at thalamocortical synapses contributes to rapid adaptation of cortical sensory responses in vivo. Neuron *34*, 437–446.

Crochet, S., and Petersen, C.C.H. (2006). Correlating whisker behavior with membrane potential in barrel cortex of awake mice. Nat. Neurosci. *9*, 608–610.

Derdikman, D., Hildesheim, R., Ahissar, E., Arieli, A., and Grinvald, A. (2003). Imaging spatiotemporal dynamics of surround inhibition in the barrels somatosensory cortex. J. Neurosci. *23*, 3100–3105.

Fanselow, E.E., and Nicolelis, M.A.L. (1999). Behavioral modulation of tactile responses in the rat somatosensory system. J. Neurosci. *19*, 7603–7616.

Fee, M.S., Mitra, P.P., and Kleinfeld, D. (1997). Central versus peripheral determinants of patterned spike activity in rat vibrissa cortex during whisking. J. Neurophysiol. *78*, 1144–1149.

Feldman, D.E., and Brecht, M. (2005). Map plasticity in the somatosensory cortex. Science *310*, 810–815.

Ganguly, K., and Kleinfeld, D. (2004). Goal-directed whisking increases phase-locking between vibrissa movement and electrical activity in primary sensory cortex in rat. Proc. Natl. Acad. Sci. USA *101*, 12348–12353.

Grinvald, A., and Hildesheim, R. (2004). VSDI: a new era in functional imaging of cortical dynamics. Nat. Rev. Neurosci. *5*, 874–885.

Grinvald, A., Anglister, L., Freeman, J.A., Hildesheim, R., and Manker, A. (1984). Real-time optical imaging of naturally evoked electrical activity in intact frog brain. Nature *308*, 848–850.

Grinvald, A., Lieke, E., Frostig, R.D., Gilbert, C.D., and Wiesel, T.N. (1986). Functional architecture of cortex revealed by optical imaging of intrinsic signals. Nature *324*, 361–364.

Helmchen, F., Fee, M.S., Tank, D.W., and Denk, W. (2001). A miniature head-mounted two-photon microscope: high resolution brain imaging in freely moving animals. Neuron *31*, 903–912.

Hentschke, H., Haiss, F., and Schwarz, C. (2005). Central signals rapidly switch tactile processing in rat barrel cortex during whisker movements. Cereb. Cortex, in press. Published online October 12, 2005. 10.1093/cercor/bhj056.

Higley, M.J., and Contreras, D. (2005). Integration of synaptic responses to neighboring whiskers in rat barrel cortex in vivo. J. Neurophysiol. *93*, 1920–1934.

Holtmaat, A.J., Trachtenberg, J.T., Wilbrecht, L., Shepherd, G.M., Zhang, X., Knott, G.W., and Svoboda, K. (2005). Transient and persistent dendritic spines in the neocortex in vivo. Neuron *45*, 279–291.

Keller, A., and Carlson, G.C. (1999). Neonatal whisker clipping alters intracortical, but not thalamocortical projections, in rat barrel cortex. J. Comp. Neurol. *412*, 83–94.

Kelly, M.K., Carvell, G.E., Kodger, J.M., and Simons, D.J. (1999). Sensory loss by selected whisker removal produces immediate disinhibition in the somatosensory cortex of behaving rats. J. Neurosci. *19*, 9117–9125.

Kleinfeld, D., and Delaney, K.R. (1996). Distributed representation of vibrissa movement in the upper layers of somatosensory cortex revealed with voltage-sensitive dyes. J. Comp. Neurol. *375*, 89–108.

Krupa, D.J., Wiest, M.C., Shuler, M.G., Laubach, M., and Nicolelis, M.A.L. (2004). Layer-specific somatosensory cortical activation during active tactile discrimination. Science *304*, 1989–1992.

Moore, C.I., and Nelson, S.B. (1998). Spatio-temporal subthreshold receptive fields in the vibrissa representation of rat primary somatosensory cortex. J. Neurophysiol. *80*, 2882–2892.

Nguyen, Q.T., and Kleinfeld, D. (2005). Positive feedback in a brainstem tactile sensorimotor loop. Neuron *45*, 447–457.

Orbach, H.S., Cohen, L.B., and Grinvald, A. (1985). Optical mapping of electrical activity in rat somatosensory and visual cortex. J. Neurosci. *5*, 1886–1895.

Petersen, C.C.H., Grinvald, A., and Sakmann, B. (2003a). Spatiotemporal dynamics of sensory responses in layer 2/3 of rat barrel cortex measured in vivo by voltage-sensitive dye imaging combined with

whole-cell voltage recordings and anatomical reconstructions. J. Neurosci. *23*, 1298–1309.

Petersen, C.C.H., Hahn, T.T.G., Mehta, M., Grinvald, A., and Sakmann, B. (2003b). Interaction of sensory responses with spontaneous depolarization in layer 2/3 barrel cortex. Proc. Natl. Acad. Sci. USA *100*, 13638–13643.

Petersen, R.S., Panzeri, S., and Diamond, M.E. (2001). Population coding of stimulus location in rat somatosensory cortex. Neuron *32*, 503–514.

Polley, D.B., Chen-Bee, C.H., and Frostig, R.D. (1999). Two directions of plasticity in the sensory-deprived adult cortex. Neuron *24*, 623–637.

Polley, D.B., Kvasnak, E., and Frostig, R.D. (2004). Naturalistic experience transforms sensory maps in the adult cortex of caged animals. Nature *429*, 67–71.

Sakai, R., Repunte-Canonigo, V., Raj, C.D., and Knopfel, T. (2001). Design and characterization of a DNA-encoded, voltage-sensitive fluorescent protein. Eur. J. Neurosci. *13*, 2314–2318.

Seidemann, E., Arieli, A., Grinvald, A., and Slovin, H. (2002). Dynamics of depolarization and hyperpolarization in the frontal cortex and saccade goal. Science *295*, 862–865.

Shoham, D., Glaser, D.E., Arieli, A., Kenet, T., Wijnbergen, C., Toledo, Y., Hildesheim, R., and Grinvald, A. (1999). Imaging cortical dynamics at high spatial and temporal resolution with novel blue voltage-sensitive dyes. Neuron *24*, 791–802.

Siegel, M.S., and Isacoff, E.Y. (1997). A genetically encoded optical probe of membrane voltage. Neuron *19*, 735–741.

Simons, D.J. (1985). Temporal and spatial integration in the rat SI vibrissa cortex. J. Neurophysiol. *54*, 615–635.

Slovin, H., Arieli, A., Hildesheim, R., and Grinvald, A. (2002). Long-term voltage-sensitive dye imaging reveals cortical dynamics in behaving monkeys. J. Neurophysiol. *88*, 3421–3438.

Spors, H., and Grinvald, A. (2002). Spatio-temporal dynamics of odor representations in the mammalian olfactory bulb. Neuron *34*, 301–315.

Szwed, M., Bagdasarian, K., and Ahissar, E. (2003). Encoding of vibrissal active touch. Neuron *40*, 621–630.

Woolsey, T.A., and Van der Loos, H. (1970). The structural organisation of layer IV in the somatosensory region (SI) of the mouse cerebral cortex: the description of a cortical field composed of discrete cytoarchitectonic units. Brain Res. *17*, 205–242.

Zhu, J.J., and Connors, B.W. (1999). Intrinsic firing patterns and whisker-evoked synaptic responses of neurons in the rat barrel cortex. J. Neurophysiol. *81*, 1171–1183.